Laboratory Measurements of Spontaneous Oscillations for Moderate-Size Raindrops

RODNEY J. KUBESH AND KENNETH V. BEARD*

Illinois State Water Survey, Cloud and Precipitation Research, Champaign, Illinois

(Manuscript received 15 October 1991, in final form 26 May 1992)

ABSTRACT

The natural oscillations of moderate-size raindrops were studied in a seven-story fall column using a computer-controlled generator to produce isolated water drops at terminal speed. Instantaneous shapes were photographed to obtain oscillation sequences of single drops by a multiple-strobe technique. The oscillation frequencies were determined from fall-streak modulations that were photographed in backscattered light of the primary rainbow. Measurements were made at three levels for 2.0- and 2.5-mm diameter drops to assess the role of aerodynamic feedback as the source of drop oscillations.

Variations as large as 15% in axis ratio were observed at the bottom of the fall column, even though the initial oscillations were predicted to die out by viscous decay theory. Practically all oscillations were at the fundamental and first harmonic frequencies. The oscillation modes deduced from the axis ratio scatter indicated that the axisymmetric modes died away slowly and that transverse modes persisted. The slow decay of the axisymmetric modes is postulated to be caused by positive feedback of shape-induced changes in pressure and drag from the initial oscillations. The transverse mode is believed to persist because of transverse pressure perturbations associated with eddy shedding. Various types of feedback are considered that could explain the broad coupling between eddy shedding and oscillations.

The mean experimental axis ratios were higher than equilibrium values—an apparent consequence of shape changes from transverse modes. The deviation from equilibrium shape was generally consistent with previous field measurements of raindrop axis ratios. Use of empirical mean axis ratios in differential reflectivity calculations would change equilibrium values of Z_{DR} by 20%–30%.

1. Introduction

The shape of raindrops has been studied since the time of Lenard. He noted raindrop distortion from flash observations in nocturnal rainfall and made extensive laboratory measurements of drop shape and oscillations (Lenard 1887, 1904). Somewhat later, Schmidt (1913) made visual observations of raindrop oscillations in backscattered sunlight. Quantitative measurements of raindrop shape were obtained using orthogonal cameras by Jones (1959), who found a large scatter in raindrop axis ratio for sizes from 2 to 6 mm diameter as a result of large amplitude oscillations. Volz (1960) photographically determined that raindrops of diameter 0.4 to 1.5 mm were oscillating using the method of Schmidt.

Water drops have been observed to oscillate in the oblate–prolate mode in numerous wind tunnel studies as an apparent consequence of turbulence or shear (e.g., Blanchard 1950; Brook and Latham 1968). Brook and Latham found mean and extreme axis ratios for 4–6-mm diameter water drops that are remarkably similar to the raindrop observations of Jones [see comparison in Beard (1984)]. Both the wind tunnel and field results showed that mean axis ratios are shifted significantly from axis ratios for nonoscillating drops (Pruppacher and Beard 1970) as a likely consequence of bias from oblate–prolate oscillations (Foote 1972; Beard 1984). The cause of oscillations for such large raindrops is unlikely to be shear, but rather drop collisions that can occur frequently enough in heavy rainfall to maintain raindrop oscillations (Beard et al. 1983).

Recent field studies have provided additional evidence of raindrop oscillations for 1–3-mm diameter (Chandrasekar et al. 1988; Sterlyadkin 1988; Beard and Tokay 1991) in situations where drop collisions might not be expected to play a significant role. The source of these oscillations may be eddy shedding in the wake. This phenomenon has been investigated in our laboratory for water drops of 0.7–1.5-mm diameter falling at terminal speed (Beard et al. 1989b, 1991; Beard and Kubesh 1991). We also noted a displacement in the average axis ratio for 1.0–1.5-mm diameter raindrops as a consequence of transverse mode oscillations. This mode was attributed to forcing by eddies detaching alternately from opposite sides of the upper pole.

An important aspect of these studies is that the average axis ratio of oscillating raindrops is generally dif-

* Also affiliated with Department of Atmospheric Sciences, University of Illinois, Urbana, IL.

Corresponding author address: Dr. Kenneth V. Beard, Department of Atmospheric Sciences, University of Illinois, 105 South Gregory Avenue, Urbana, IL 61801.

ferent than the equilibrium shape. The change in distortion can be significant (Jones 1959; Beard et al. 1983). For example, the differential polarization radar signal Z_{DR} (Seliga and Bringi 1976) is altered by up to 30% (at zero elevation angle), leading to erroneous estimates of drop size and rainfall rate. Thus, it is important for microwave scattering applications to determine and predict raindrop shape changes caused by oscillations. This requires controlled studies of raindrop oscillations.

Here we report on research where we have extended our laboratory studies to moderate-size raindrops of 2.0- and 2.5-mm diameter. Water drops were generated at terminal speed with a computer-controlled system and descended a seven-story (25.6 m) fall column under free-fall conditions, allowing investigation of oscillations over large distances. Drop axis ratios were measured from stroboscopic photographs, and oscillation frequencies were determined from modulations of fall streaks in backscattered light.

2. Background

Oscillations are well represented by spherical-harmonic perturbations (e.g., Pruppacher and Klett 1978) of sinusoidal amplitude with frequencies given by

$$f_n = [2n(n-1)(n+2)\gamma]^{1/2}[\pi^2\rho d^3]^{-1/2} \quad (1)$$

for drops of density ρ, surface tension γ, and diameter d (where d is the diameter of an equivalent volume sphere). The fundamental frequency corresponds to $n = 2$ (two-lobed modes), and the first harmonic is represented by $n = 3$ (three-lobed modes). For each frequency there is one axisymmetric mode ($m = 0$) and $m = n$ physically distinct asymmetric modes. Modes of the lower order n have been identified in laboratory studies of drop oscillations [for example, see the two-liquid experiments of Trinh et al. (1982)]. Although water drops falling in air are aspherical, their oscillations appear as spherical harmonic perturbations on the raindrop equilibrium shape.

Schmidt (1913), using visual observations, determined the oscillation frequency for natural oscillations in rain. He made use of backscattered light from the primary rainbow, which is interrupted if the drop oscillates. The observed fall streaks have gaps separated by a distance $s = V/f$ for drops of fall speed V and frequency f. The fundamental frequency (f_2) and terminal fall speed must be assumed in order to determine the size of oscillating drops from photographic measurements of s (Volz 1960; Sterlyadkin 1988). In our recent laboratory work (Beard and Kubesh 1991) we made measurements of f for water drops of known size under free-fall conditions. Both the fundamental and first harmonic were observed for the drop sizes studied (diameter ranging from 1.04 to 1.54 mm) in the form of axisymmetric ($m = 0$) and transverse modes ($m = 1$). These laboratory results indicate raindrops do not necessarily oscillate only at the fundamental frequency.

In our laboratory experiments we generate water drops at terminal velocity that are initially oscillating (because of jet breakup) with large amplitude and many oscillation modes. These initial oscillations were allowed to decay through viscous dissipation so that only naturally forced oscillations would be observed. The distance needed for the initial oscillation to damp to a negligible amount can be readily calculated from Lamb's theory for the viscous damping of free oscillations of a liquid sphere (Beard et al. 1991). The oscillation amplitude of a liquid sphere decays exponentially in time, and the time constant is largest for the fundamental frequency. Table 1 indicates the fall distance needed for an $n = 2$ oscillation to decay to the negligible amplitude. These amplitudes are a conservative limit, since the damping is aided by vorticity diffusion (Prosperetti 1977). An initial axis ratio of 0.65 was chosen, based on the typical oblate distortion observed directly below the drop generator. Observations of natural drop shapes were done far enough below the generator so that any residual amplitude would be a negligible factor in the measurements.

Table 1 shows why it was necessary to conduct the experiment for moderate size drops in a seven-story (25.6 m) stairwell. For a 2.5-mm drop, the original amplitude does not damp to a negligible level until it has fallen at least three floors (11.0 m). Once the original amplitude has decayed to a very small amount, axis ratio measurements can be made at that position and one or more floors below to verify the existence of natural, self-excited oscillations and to investigate the oscillation behavior over large fall distances.

If the original amplitude does not decay as predicted, then aerodynamic forcing by eddy shedding or drag forcing are plausible. These types of feedback are discussed below.

Eddy shedding. The flow around a moderate-size raindrop is unsteady above a critical Reynolds number of about 300 ($d \approx 1$ mm). This phenomenon is well documented for a sphere; it appears as a series of wake transitions, from steady, attached flow to the shedding of regions of fluid with concentrated vorticity (Ma-

TABLE 1. Axis-ratio amplitude at the indicated descent. Calculations were made for the viscous damping of a water sphere oscillating at $n = 2$ with an initial axis ratio of 0.65 (dash denotes amplitude <0.001).

d (mm)	Floors of fall (3.66 m between floors)						
	1	2	3	4	5	6	7
1.5	0.001	—	—	—	—	—	—
2.0	0.022	0.001	—	—	—	—	—
2.5	0.079	0.015	0.003	0.001	—	—	—
3.0	0.140	0.050	0.017	0.006	0.002	0.001	—

garvey and Bishop 1961). The periodic detachment of eddies in the drop wake is thought to excite drop vibrations through induced pressure changes at the drop surface, possibly resulting in resonance between the eddy-shedding frequency and a natural frequency of the drop. Beard et al. (1991) confirmed the presence of eddy-induced oscillations for small raindrops falling at terminal velocity. More information on drop wakes can be found in their paper.

Drag forcing. The shape variations of an oscillating drop will cause changes in drag. Consider again an oblate–prolate oscillation. A drop becoming more oblate will decelerate because of the increased drag coefficient. This deceleration will produce an increase in the hydrostatic pressure (Beard 1977), further distorting the drop and enhancing the oscillation. Calculations based on the potential energy model of Beard (1984) show that the effect should be a substantial one. The relationship between drop shape and acceleration was determined using measured drag coefficients for spheroids of various axis ratios, and the instantaneous accelerations at the oscillation endpoints were found to be a considerable fraction of 1 g (the amount in the equilibrium distortion). Thus, drag forcing is also a potentially significant positive feedback to axisymmetric oscillations.

3. Experiment

Figure 1 is a schematic of the experimental apparatus. The system used to generate drops consisted of a water supply, orifice-jet drop generator, charging electrode, electrostatic deflection chamber with digital circuits controlled by an IBM-compatible PC. A discussion of the drop generator controls can be found in Czys and Ochs (1988).

Filtered tap water for drop generation was supplied under low pressure from epoxy-lined steel tanks (after degassing overnight in a partial vacuum). The water tanks and drop generator were placed on a vibration-isolation platform to improve the stability of drop generation. Capillary waves were excited on the water jet by a piezoelectric transducer causing the jet to break up into uniform-size drops. Most drops were charged by the concentric electrode and deflected to a drain by a high-voltage field. Periodically the electrode voltage was pulsed off, allowing only isolated drops to enter the velocity measurement section. Charges on these undeflected drops were negligible with respect to surface stresses (i.e., shape effects), since even those on the deflected drops were well below the Rayleigh bursting limit.

Drop velocities were measured just below the drop generator section (see Fig. 1) from the transit time between two horizontal laser beams 25 cm apart. If necessary, the water pressure was adjusted so that a drop would achieve terminal speed (±1%) within a few additional meters of fall, as determined by acceleration calculations.

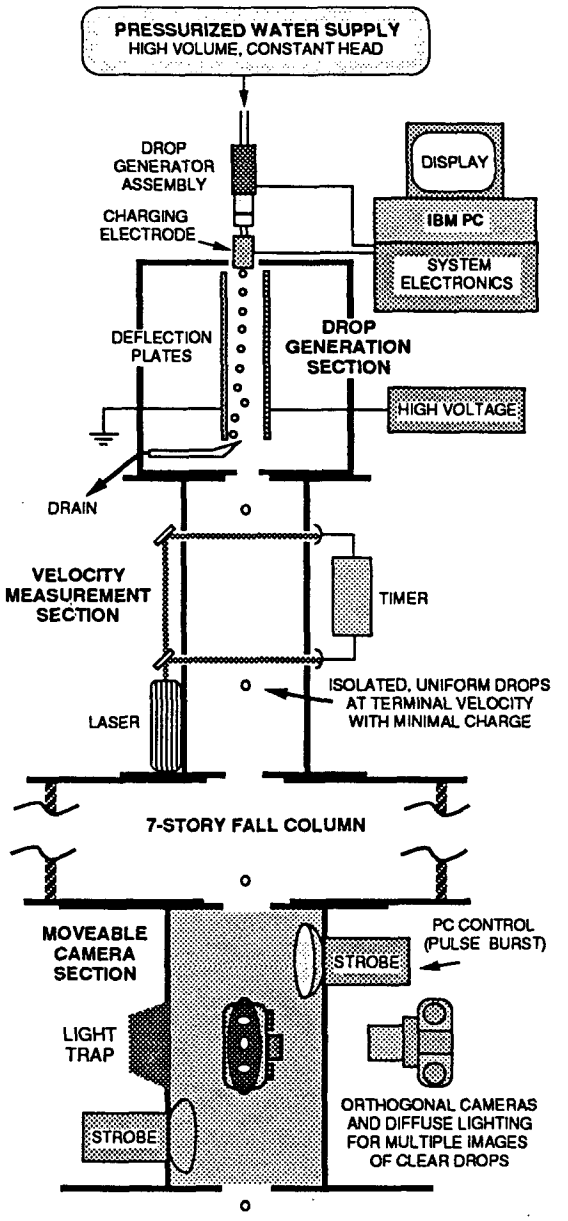

FIG. 1. Schematic of seven-story experiment for measuring the oscillation shapes and frequencies of drops at terminal velocity. Filtered water at a constant head is supplied from storage tanks, forced through an orifice, and caused to break into uniform-size drops by a coaxial transducer. The charging electrode and high voltage plates are used to deflect most drops to obtain isolated, uncharged drops. The fall speed is determined from the transit time between laser beams, and the flow rates adjusted to generate drops at terminal speed. Drop shapes are recorded at the camera section after falling one to seven stories. The frequency is obtained from fall streaks on film using another camera section (not shown).

Upon exiting the velocity measurement section, the drops entered a fall column in a seven-story stairwell. The gap between the railings provided a convenient

space for the fall column, which consisted of flexible ducts 46 cm diameter and 3.7 m long, one section hung from each floor. As was the case with smaller drops, the drops drifted horizontally (see Beard et al. 1991), so the drops had to be aimed to descend the fall column without hitting it.

In the stairwell there was a stable temperature gradient with the top being about 5°C warmer than the bottom. In the fall column the average temperature and relative humidity varied from day to day, depending on outside temperature, over the range 17°–23°C and 70%–90%.

The bottom of each flexible duct at every floor could be lifted to allow installation of the camera units used for the axis ratio measurements. For multiple-image photographs of a single drop, a camera unit was made from an assembly of PVC pipe sections lined with crinkled aluminum foil. Openings were cut for four strobe lights and two orthogonal cameras with light traps. The strobes were fired simultaneously in a burst of 5 to 15 flashes to obtain multiple-image photographs of single drops. For each strobe flash the clear drop acted as a lens, inverting the surroundings. Thus, a well-defined drop shape was recorded because of the high contrast between the dark background and the edge of the drop showing an image of the illuminated surroundings. Multiple images were possible because of the dark background.

We used 35-mm cameras with 50-mm macro lenses, power winders, and data backs. The new Kodak T-grain black and white films (TMAX 400 or 3200) were found to be the best compromise between the requirements of a fast film and a fine grain for good resolution. Our photographic method yielded drop images with distinct edges as long as the drop was in focus. Many images were out of focus because of insufficient depth of field (a large lens aperture was required because of low illumination; the strobe intensity could not be increased without lowering the flash rate).

Because of the small drop sizes and low camera magnifications, the negatives were placed under a low-power microscope, where a filar eyepiece micrometer was used to measure the horizontal and vertical dimensions h and v for calculation of the axis ratio, $\alpha = v/h$. A drop image was passed over if the focus was so poor that the drop edge could not be located with confidence. Sources of error in the measurements were 1) uncertainty inherent in the scale of the eyepiece micrometer, which was about 1/2%, and 2) error from imperfectly defined drop edges due to film grain and less-than-optimal focus. The film grain was not a problem for drops in good focus. These measurement errors were not very large; the appropriate measure of the uncertainty, the standard deviation of the axis ratio, was typically 0.007 (less than 1% of the mean axis ratio).

To obtain frequency data, fall streaks were recorded on TMAX 3200 film as drops fell through a large light trap placed in the column (not shown in Fig. 1). The camera was positioned about 3 meters from the light trap at the same height. The drops were illuminated by a dc spotlight above the camera at the angle of the primary rainbow. The eyepiece micrometer on the microscope was used to determine the spacing of the interrupted fall streaks so that the frequency, $f = V/s$, could be calculated from s and the known fall speed V. A detailed description of the rainbow technique is found in Beard and Kubesh (1991). To facilitate comparison of our findings with results from other liquid drop systems, information on our experimental parameters is provided in Table 2.

4. Results

a. Axis ratios

The oscillation behavior was investigated for 2.0- and 2.5-mm diameter drops with sizes maintained to within 2% during or between experiments. For both sizes, photographs were taken at three levels yielding a total of six datasets. Measurements of 2.0-mm size were made at one, two, and seven floors of fall (corresponding to fall heights of H = 3.7 m, 7.3 m, and 25.6 m). (These results are referred to as datasets 2A, 2B, and 2C, respectively.) Table 1 shows that the oscillation amplitude for a 2.0-mm drop should have decayed to an insignificant amount by the second level. Measurements of the 2.5-mm size were made at two, three, and seven floors of fall (corresponding to fall heights H = 7.3 m, 11.0 m, and 25.6 m, and referred to as datasets 2.5A, 2.5B, and 2.5C). Table 1 shows that the initial amplitude should have decayed to a negligible amount by the second measurement level (at the third floor).

For the axis-ratio measurements a subjective estimation was made of the focus quality of each image, with five categories ranging from "poor" to "excellent." After the axes were all measured, we decided that the two lowest categories had unacceptable variances due to indistinct edges. Therefore, the axis-ratio results are

TABLE 2. Information on experimental parameters at 20°C and 1 atmosphere. Dimensional parameters are drop diameter (d), terminal velocity (U), and oscillation frequency of the fundamental (f_2) and first harmonic (f_3). Nondimensional parameters are Reynolds number ($\mathrm{Re} = \rho d U/\eta$), Weber number ($\mathrm{We} = \rho_L U^2 d/\gamma$), and Strouhal number ($\mathrm{St}_n = fd/U$), where η is the viscosity of air and ρ_L is the density of water.

Dimensional parameters			Nondimensional parameters		
	d (mm)			Re	
	2.0	2.5		86	1221
U (cm s^{-1})	654	740	We	1.41	2.25
f_2	122	87.1	St_2	0.0372	0.0294
f_3	236	68.7	St_3	0.0721	0.0570

TABLE 3. Experimental measurements of axis ratio ($\bar{\alpha}$, α_{min}, α_{max}). Also shown is the fall height (H), equilibrium axis ratio (α_{eq}), axis ratio range ($\Delta\alpha = \alpha_{max} - \alpha_{min}$), sample standard deviation (σ), number of measurements (N), and the 95% confidence interval in the mean.

Dataset	H (m)	α_{eq}	$\bar{\alpha}$	α_{min}	α_{max}	$\Delta\alpha$	σ	N	95% C.I.
				d = 2.0 mm					
2A	3.7	0.929	0.950	0.902	1.003	0.101	0.022	119	0.946–0.954
2B	7.3	0.929	0.944	0.897	0.983	0.086	0.019	58	0.939–0.949
2C	25.6	0.929	0.953	0.928	1.000	0.072	0.018	43	0.948–0.958
				d = 2.5 mm					
2.5A	7.3	0.892	0.917	0.878	0.976	0.098	0.022	118	0.913–0.921
2.5B	11.0	0.892	0.924	0.891	0.957	0.066	0.015	42	0.919–0.929
2.5C	25.6	0.892	0.923	0.867	0.984	0.117	0.020	60	0.918–0.928

given for only the three highest categories. These data are summarized in Table 3. The mean and extremes of these data are plotted in Fig. 2 along with 95% confidence intervals and the theoretical curve for the equilibrium axis ratio (Beard et al. 1989a).

In all cases there are large variations in axis ratio as well as a shift of the mean axis ratio away from the equilibrium value, indicating the presence of oscillations. The 2.0-mm size has axis ratios with means that vary from 0.944 to 0.953 and extreme values ranging from 0.897 to 1.003. The standard deviation (σ) shown in Table 3 is comprised of two components: the uncertainty due to experimental error (σ_{error}) and the variability due to oscillations (σ_{osc}); $\sigma = \sqrt{\sigma_{error}^2 + \sigma_{osc}^2}$. These standard deviations were comparable for the three datasets, averaging about 0.02. Since the experimental error is relatively small ($\sigma_{error} \approx 0.007$), σ_{osc} is nearly equal to σ in all cases and was approximately 2% of the equilibrium axis ratio. For the 2.5-mm size the mean varied between 0.917 and 0.924 with extremes of 0.867 and 0.984, and σ_{osc} was again around 2% of the equilibrium axis ratio.

Histograms of the number of observations per 0.01 axis ratio interval are shown in Figs. 3 and 4. For datasets 2A, 2B, and 2.5A, a significant fraction of the axis ratios falls below the equilibrium value α_{eq}, while for the rest of the data, almost all the axis ratios lie above α_{eq} (except for one data point each for 2C, 2.5B, and 2.5C). Beard and Kubesh (1991) showed, through geometric analysis of the spherical harmonic profiles for the modes of the fundamental and first harmonic (n = 2 and n = 3), that the only mode with axis ratios that scatter exclusively *above* the equilibrium curve is the transverse mode (m = 1). It appears, then, that all data for the lowest level can be attributed to transverse mode oscillations, while the data for the top level must also contain some axisymmetric mode oscillations, for which the axis ratios vary both above and below equilibrium.

The axisymmetric mode in the 2B and 2.5B data persists longer than expected from viscous decay (see Table 1), indicating a positive feedback, possibly from drag forcing, as complete damping was retarded by several floors. The presence of transverse modes at the lowest level is consistent with the spatial pattern of the forcing due to eddy shedding on opposite sides of the upper pole of the drop. This may indicate that equilibrium oscillations have been achieved with the aerodynamic feedback from eddy shedding. From our observations we conclude that times much longer than viscous decay are needed before the oscillations induced by the drop generator, or by drop collisions, die away.

We assessed the possibility that the observed distributions might have been sampled from a normal distribution about the equilibrium axis ratio using a chi-square test. In each case the probability of such an occurrence was less than 1%, indicating that the shifted distributions were not merely chance events.

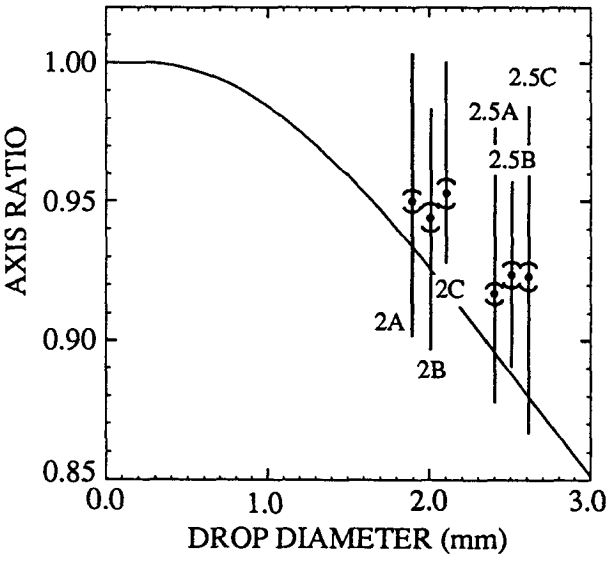

FIG. 2. Mean axis ratios at three levels for each drop size compared to equilibrium (solid line). The range of axis ratios is indicated by vertical bars, and the 95% confidence intervals for the mean are outlined by arcs. Data points for A and C are displaced horizontally to avoid overlap.

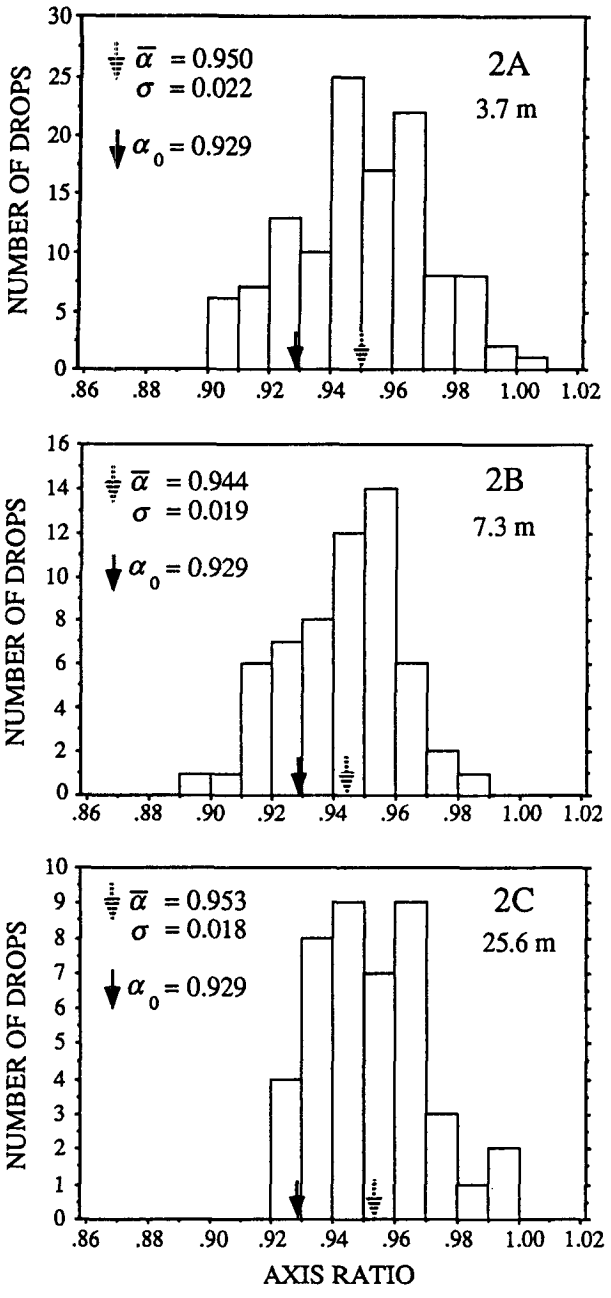

FIG. 3. Histograms of axis ratios for 2.0-mm diameter data with number of drops given in 0.01 intervals of axis ratio. The equilibrium axis ratio is shown by a black arrow and the mean axis ratio by a striped arrow.

The peak of the axis-ratio distribution is near the mean in all cases. The distribution for equal-amplitude oscillations, however, should have the greatest number of observations near the extreme values, since the most time is spent near the turning points. For the axisymmetric mode the distribution would be saddle shaped, unlike Figs. 3 and 4. Equal-amplitude transverse oscillations should be shaped like half a saddle, since the axis ratios only scatter on one side of the equilibrium value. Therefore, our observed axis-ratio distributions indicate a variety of oscillation amplitudes with most amplitudes less than the extremes shown. This question can be analyzed in a more rigorous way using probability density functions (Kubesh 1991).

b. Oscillation frequencies

To determine the oscillation length s, the center of the dark gap was found and the distance between two consecutive centers was measured. This distance was

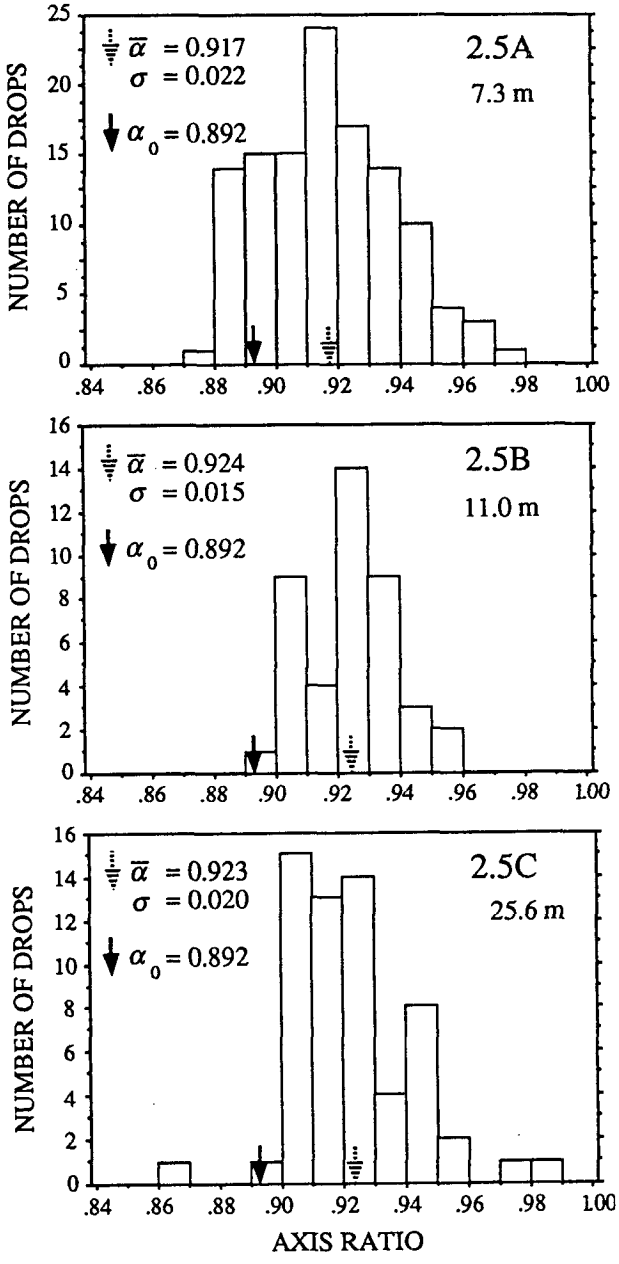

FIG. 4. As in Fig. 3 but for 2.5-mm diameter data.

converted to centimeters using a calibration factor found from photographs of a meter stick placed in the light trap, allowing calculation of the frequency $f = V/s$, where V is the terminal velocity. Not all streaks had distinct gaps due to insufficient amplitudes or low light intensities. In such cases, s could not be measured. A close examination of these cases revealed that practically all had at least one modulation, indicating small oscillation amplitudes rather than none at all.

The frequency distributions shown in Figs. 5 and 6 are bimodal, with one peak near the fundamental frequency f_2 and the other at about twice the fundamental, near the first harmonic $f_3 = 1.94f_2$. Thus, the data were stratified into two groups based on f_2 and f_3, and the means and standard deviations are given in Figs. 5 and 6. The means, standard deviations, and number of data points are listed in Table 4. There are only two levels for the 2.0-mm size as no frequency measurements were made at the first level (3.7 m). The Student's t distribution was used to test, at the 5% significance level, whether the mean for each dataset $\bar{f}$ is consistent

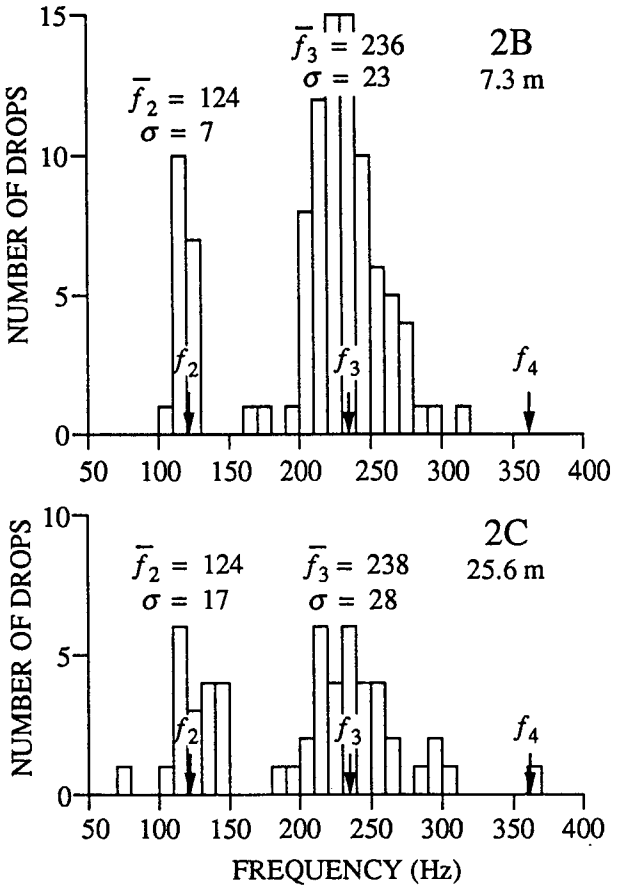

FIG. 5. Histograms of frequency for 2.0-mm diameter data at two levels (fall distances) with number of drops given in 10-Hz intervals of frequency. The means and standard deviations for the lower harmonics are specified in Hertz, and the corresponding theoretical frequencies are designated by arrows on the x axis.

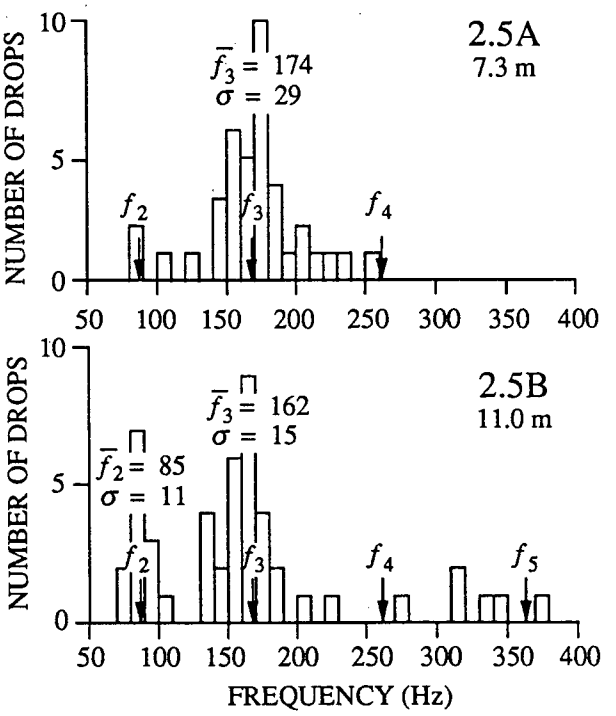

FIG. 6. As in Fig. 5 but for 2.5-mm diameter data.

with the hypothesis that $\bar{f} = f_2$ or $\bar{f} = f_3$, as the case may be. All averages were found to be consistent with Eq. (1), except for one where the discrepancy was still within the uncertainty in the measurement.

After the frequency data were obtained, the fall streaks were investigated theoretically by calculating the light intensity as a function of the drop's vertical coordinate using geometric optics. The relative intensity for monochromatic light undergoing one internal reflection was calculated as a function of emergence angle. An oblate–prolate oscillation was assumed for which the drop is ellipsoidal and its cross section an ellipse. The calculations were repeated for successive positions in the drop's descent at terminal velocity using 16 steps per oscillation period. The amount of the rainbow angle deviation was quantified by the formula of Möbius (1910). Input parameters for the program were the drop fall speed, oscillation period, oscillation amplitude, and equilibrium axis ratio, along with the distances between the lamp, drop, and camera. Since the light was not a point source, rays arrived at the drop over a finite angle; this had the effect of smoothing out the intensity fluctuations (when different colors were included, it also caused color mixing). The calculated fall streaks showed that the dashes, separated by a distance $s = V/f$, were more pronounced with increasing oscillation amplitude and that the intensity of the dashes increased as the light–drop–camera angle approached the rainbow angle. We also found that the vertical extent of the dashes increases with amplitude

TABLE 4. Mean oscillation frequency ($\bar{f}_2, \bar{f}_3$) for each drop size (d) at each experimental fall distance (H) stratified into two groups based on theoretical frequencies f_2 and f_3. Also shown are the standard deviation (σ) and the number in each sample (n).

d (mm)	H (m)	f_2 (Hz)	$\bar{f}_2$ (Hz)	σ	n	f_3 (Hz)	$\bar{f}_3$ (Hz)	σ	n
2.0	7.3	122	124	7	20	236	236	23	79
2.0	25.6	122	124	17	19	236	238	28	34
2.5	7.3	87	88	2	3	169	174	29	36
2.5	11.0	87	85	11	13	169	162	15	28
2.5	25.6	87	93	0	1	169	203	31	4

in a predictable way. Thus, oscillation amplitudes for various modes and orientations can be determined from the fall-streak data using our code. Amplitude information cannot be obtained from the present data, however, because we did not record the entire portion of the dashed streaks. This can be rectified in future experiments by simply illuminating and photographing a larger area centered on the primary rainbow for the drop size of interest.

5. Discussion

a. Axis ratios

Our axis-ratio results are plotted in Fig. 7 for each size after combining the data from all three levels. The data points give mean values ($\bar{\alpha}$) and the vertical bars denote sample standard deviations (σ). Also plotted are data from Beard et al. (1991), Jones (1959), Chandrasekar et al. (1988), and Sterlyadkin (1988). One curve is shown for equilibrium axis ratios and another for the shifted axis ratios postulated by Goddard and Cherry (1984). The latter were devised to rectify values of Z_{DR} measured with a high-resolution radar and values calculated from raindrop size distributions measured by disdrometer.

The average axis ratios for the combined data at 2.0- and 2.5-mm diameter are $\bar{\alpha} = 0.949$ and 0.920, respectively. Values for these sizes from Chandrasekar et al. are $\bar{\alpha} = 0.950$ and 0.913 (estimated from their Fig. 5g), whereas values from Goddard and Cherry are $\bar{\alpha} = 0.945$ and 0.904. By using the normal deviate test (Meyer 1975), we found that our mean axis ratios were likely to have come from the same population as those of Chandrasekar et al. (at the 5% significance level). In a similar comparison, the data of Jones (1959) for 2.0 and 2.5 mm ($\bar{\alpha} = 0.983$ and 0.975) were found to be from a different population. These higher mean axis ratios may be from other causes, such as oscillations induced by collisions (Beard et al. 1983), since the data were obtained for high rainfall rates in thunderstorms (Jones, personal communication).

Goddard and Cherry's axis ratios are shifted in the same sense as our results out to $d = 3$ mm. Not enough information is available to perform a normal deviate comparison with their results, but their values for 2.0 and 2.5 mm lie very close to ours. Sterlyadkin (1988) also reports measurements of axis ratio. He did not have data points at our two sizes but provided an empirical equation: $\alpha = 1.0 - 0.016d - 0.07d^2$ (d in centimeters), which gives $\alpha = 0.940$ and 0.898 for 2.0 and 2.5 mm, respectively. Since his values lie outside the 95% confidence intervals for our data, his results may be significantly lower.

b. Oscillation frequencies and modes

In our experiments, drops were found to oscillate at the lower two levels, even though viscous decay theory predicts that oscillation should have been negligible.

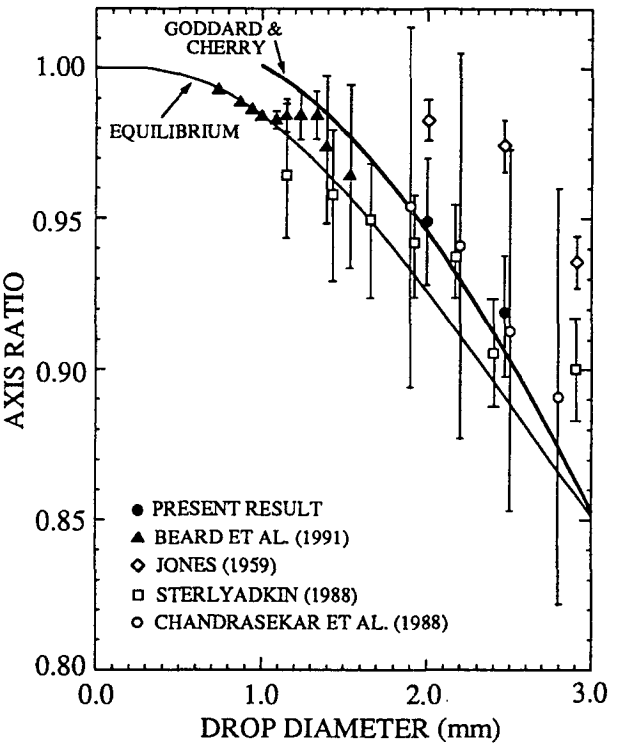

FIG. 7. Observed raindrop distortion as a function of size. The mean axis ratios for the present experiment are given by the solid circles with the standard deviation indicated by vertical bars. Means and standard deviations are also plotted for the data of Beard et al. (filled triangles), Jones (open diamonds), Chandrasekar et al. (open circles), and Sterlyadkin (open squares). Also shown is the empirical axis ratio curve postulated by Goddard and Cherry (1984) and the equilibrium axis-ratio curve of Beard et al. (1989a).

Such observations show that external forcing acts in opposition to viscous dissipation. The shift in mean axis ratio and the dominance of the transverse mode indicate that the forcing arises from resonance with the shedding of eddies in the drop wake, in agreement with Beard et al. (1991). Resonant oscillations extend far beyond the 1-mm size originally proposed by Gunn (1949), however, as large axis ratio variations are observed even for $d = 2.5$ mm. Oscillations for raindrops this large are generally believed to originate from collisions (e.g., Chandrasekar et al. 1988), but the results of our study indicate that oscillations of moderately sized raindrops are affected by aerodynamic feedback as well. Such feedback may prolong axisymmetric oscillation induced by collisions and promote steady-state oscillations induced by eddy shedding.

The largest amplitude steady-state oscillations should occur when the natural frequency of the drop matches the eddy-shedding frequency, producing resonance. A large mismatch seems to exist, however, between the oscillation and eddy-shedding frequencies for 2.0- and 2.5-mm drops based on results for spheres (Möller 1938; Achenbach 1974). Even the new, lower-frequency regime for eddy shedding found by Kim and Durbin (1988) for spheres indicates eddy-shedding frequencies for 2.0- and 2.5-mm drops exceed f_2 by factors of 3.5 and 7, respectively, and f_3 by factors of 3 and 5. Several factors may aid oscillations despite poor frequency matching. Subharmonic resonance can occur if the eddy-shedding frequency is equal to some integer multiple of f_2 or f_3 (Feng and Beard 1991a,b). In addition, pressure changes at the drop surface resulting from the changing shape may trigger the instability in the wake, making the frequencies come into phase with each other.

The streak photographs showed that the length of the streaks (and gaps) varied in random ways from drop to drop. For axisymmetric oscillations the dashes (and gaps) should be of rather uniform length for a given oscillation amplitude, but variations in dash length from streak to streak will occur because of variations in oscillation amplitude (as revealed by optics calculations, Kubesh 1991). Such streak variations indicate that there is a spectrum of amplitudes in our sample of drops. As discussed earlier, the axis-ratio distributions are also consistent with a spectrum of amplitudes. Observations by Schroeder and Kintner (1965) of oscillating liquid drops falling in liquid also show a large scatter in amplitude. If the eddy shedding is irregular, it would give rise to a spectrum of oscillation energies, and the amplitude of a *particular* drop may continually go through transient changes, never reaching a steady state. Another cause of modulated amplitudes is the mismatch of the forcing and oscillation frequencies. The resulting oscillations could be modulated at a beat frequency with a simple periodic amplitude, or be aperiodic or even chaotic. In any case, this is not the steady-state amplitude envisioned for a balance between aerodynamic feedback and viscous decay.

The coexistence of easily discernible oscillations and those with very small amplitude is puzzling because the drops start out with roughly the same initial conditions, in contrast to an environment where the oscillations are triggered by random collisions among drops. This sensitive dependence on initial conditions is the trademark of chaos, and its existence should not be a surprise considering the complicated nonlinear interactions possible in this fluid system.

Resonance may excite both the fundamental and first harmonic. The analysis of streak photographs by Beard and Kubesh (1991) led them to suggest that $n = 3$ may have been occasionally superimposed on $n = 2$. Evidence of superposition was also seen in the present data: two groups of dashes consisting of two dashes each were sometimes recorded, with the gap between the dashes shorter than the gap between the groups. The groups occur at the fundamental frequency, while the individual dashes repeat at the frequency of the first harmonic. Similarly, also observed were two dashes, separated by a distinct gap, that each showed intensity modulation without being broken. Similar streaks were noted by Lenard (1887), who studied drops detached from a dripper, which would be expected to show several harmonics. Superposition of the two frequencies might be explained by the reasonable notion that eddy shedding does not occur at a pure frequency but has components near multiples of both f_2 and f_3.

Feng and Beard (1991b) have examined the excitation of drop oscillations for a conducting drop in an alternating electric field to avoid the difficulties of calculating the transient flow at large Reynolds number for raindrops (see also Feng and Beard 1991a). They found that the nonlinear drop dynamics produced superharmonic, subharmonic, and coupled resonances. Large-amplitude oscillations occurred even when the forcing frequencies were displaced from the characteristic drop frequencies. The oscillation modes were not confined to those that matched the spatial pattern of the forcing. Thus, in the present experiment, modes may be excited by secondary resonances that do not match the frequencies and patterns of eddy shedding.

c. *Conclusions*

The experimental data for 2.0- and 2.5-mm diameter drops, after seven stories of fall at terminal velocity, show that the axis ratios vary but scatter only above equilibrium values. This result is consistent with the behavior of transverse mode oscillations at the fundamental and first harmonic (Beard et al. 1991). Corresponding frequency data confirm that practically all oscillations occur at these two frequencies. The transverse modes are a likely consequence of transverse forcing by eddies detaching alternately from opposite sides of the upper pole.

Our average axis ratios are remarkably close to the aircraft measurements of Chandrasekar et al. (1988) and lie only slightly above the empirical curve from the radar–disdrometer study of Goddard and Cherry (1984) and the drop camera data of Sterlyadkin (1988). [The exception is the drop camera data of Jones (1959) taken in heavy thundershowers where drop collisions could have induced stronger oscillations (Beard et al. 1983).] It is worth noting that such different approaches are in close agreement for the average axis ratios of 2.0- and 2.5-mm raindrops and that the observed shift in mean axis ratio for these sizes is equivalent to a decrease in Z_{DR} of about 30%.

We have learned from our lab studies that the oscillation behavior of falling drops is wonderfully complex. Most questions regarding the transient aspects of the oscillations remain largely unanswered. We feel fortunate to have been able to extract some useful averages of axis ratios and modes. Future studies can take several approaches. More detailed information must be obtained on the transient behaviors of oscillating drops before we can build deterministic models of raindrop shape. Measurements of axis ratio and frequencies are needed for larger drops (4 or 5 mm). Even though there are relatively few large raindrops, their contribution to radar reflectivity is appreciable because of the d^6 dependence of reflectivity. If the role of eddy shedding becomes insignificant for larger drops, it may still be necessary to characterize the transient behavior of collision-induced oscillations, especially if the decay is slowed by aerodynamic feedback. Raindrop shape should also be measured by additional field studies. Hopefully, new laboratory and field data can be synthesized to yield a more complete picture of raindrop shapes in various kinds of precipitation.

Acknowledgments. We thank Harry Ochs for his advice on experimental design and construction. This research was supported by the National Science Foundation under Grants ATM 84-19490, 86-01549, and 87-22688.

REFERENCES

Achenbach, E., 1974: Vortex shedding from spheres. *J. Fluid Mech.*, **62,** 209–221.

Beard, K. V., 1977: On the acceleration of large water drops to terminal velocity. *J. Appl. Meteor.*, **16,** 1068–1071.

——, 1984: Raindrop oscillations: evaluation of a potential flow model with gravity. *J. Atmos. Sci.*, **41,** 1765–1774.

——, and R. J. Kubesh, 1991: Laboratory measurements of small raindrop distortion. Part 2: Oscillation frequencies and modes. *J. Atmos. Sci.*, **48,** 2245–2264.

——, and A. Tokay, 1991: A field study of small raindrop oscillations. *Geophys. Res. Lett.*, **18,** 2257–2260.

——, D. B. Johnson, and A. R. Jameson, 1983: Collisional forcing of raindrop oscillations. *J. Atmos. Sci.*, **40,** 2, 455–462.

——, J. Q. Feng, and C. Chuang, 1989a: A simple perturbation model for the electrostatic shape of falling drops. *J. Atmos. Sci.*, **46,** 2404–2418.

——, H. T. Ochs, and R. J. Kubesh, 1989b: Natural oscillations of small raindrops. *Nature,* **342,** 408–410.

——, R. J. Kubesh, and H. T. Ochs III, 1991: Laboratory measurements of small raindrop distortion. Part 1: Axis ratios and fall behavior. *J. Atmos. Sci.*, **48,** 698–710.

Blanchard, D. C., 1950: The behavior of water drops at terminal velocity in air. *Trans. Amer. Geophys. Union,* **31,** 836–842.

Brook, M., and D. J. Latham, 1968: Fluctuating radar echo: Modulation by vibrating drops. *J. Geophys. Res.*, **73,** 7137–7144.

Chandrasekar, V., W. A. Cooper, and V. N. Bringi, 1988: Axis ratios and oscillations of raindrops. *J. Atmos. Sci.*, **45,** 1323–1333.

Czys, R. R., and H. T. Ochs III, 1988: The influence of charge on the coalescence of water drops in free fall. *J. Atmos. Sci.*, **45,** 3161–3168.

Feng, J. Q., and K. V. Beard, 1991a: Resonances of a conducting drop in an alternating electric field. *J. Fluid Mech.*, **222,** 417–435.

——, and ——, 1991b: A perturbation model of raindrop oscillation characteristics with aerodynamic effects. *J. Atmos. Sci.*, **48,** 1856–1868.

Foote, G. B., 1972: A numerical method for studying liquid drop behavior: Simple oscillation. *J. Comput. Phys.*, **11,** 507–530.

Goddard, J. W. F., and S. M. Cherry, 1984: The ability of dual-polarization radar (coplanar linear) to predict rainfall rate and microwave attenuation. *Radio Sci.*, **19,** 201–208.

Gunn, R., 1949: Mechanical resonance in freely falling drops. *J. Geophys. Res.*, **54,** 383–385.

Jones, D. M. A., 1959: The shape of raindrops. *J. Meteor.*, **16,** 504–510.

Kim, H. J., and P. A. Durbin, 1988: Observations of the frequencies in a sphere wake and of drag increase by acoustic excitation. *Phys. Fluids,* **31,** 3260–3265.

Kubesh, R. J., 1991: A laboratory investigation of raindrop oscillations. Ph.D. thesis, University of Illinois, Urbana–Champaign, 128 pp.

Lenard, P., 1887: Über die Schwingungen fallender Tropfen. *Ann. Phys. Chem.*, **30,** 209–243.

——, 1904: Über Regen. *Meteor. Z.*, **21,** 248–262 [for English translation see: *Quart. J. Roy. Meteor. Soc.*, **31,** 62–73 (1905).]

Magarvey, R. H., and R. L. Bishop, 1961: Wakes in liquid–liquid systems. *Phys. Fluids,* **4,** 800–805.

Meyer, S. L., 1975: *Data Analysis for Scientists and Engineers.* Wiley and Sons, 513 pp.

Möbius, W., 1910: Zur Theorie des Regenbogens und ihrer experimentellen Prüfung. *Ann. Phys.*, **33,** 1496.

Möller, W., 1938: Experimentelle Untersuchung zur Hydrodmechanik der Kugel. *Phys. Z.*, **39,** 57–80.

Prosperetti, A., 1977: Free oscillations of drops and bubbles: The initial-value problem. *J. Fluid Mech.*, **100,** 333–347.

Pruppacher, H. R., and K. V. Beard, 1970: A wind tunnel investigation of the internal circulation and shape of water drops falling at terminal velocity in air. *Quart. J. Roy. Meteor. Soc.*, **96,** 247–256.

——, and J. D. Klett, 1978: *Microphysics of Clouds and Precipitation.* D. Reidel, 714 pp.

Schmidt, W., 1913: Die Gestalt fallender Regentropfen. *Meteor. Z.*, **30,** 456–457.

Schroeder, R. R., and R. C. Kintner, 1965: Oscillations of drops falling in a liquid field. *A.I.Ch.E. J.*, **11,** 5–8.

Seliga, T. A., and V. N. Bringi, 1976: Potential use of radar differential reflectivity measurements at orthogonal polarizations for measuring precipitation. *J. Appl. Meteor.*, **15,** 69–76.

Sterlyadkin, V. V., 1988: Field measurements of raindrop oscillations. *Izvestiya, Atmos. Oceanic Phys.*, **24,** 6, 449–454.

Trinh, E., A. Zwern, and T. Wang, 1982: An experimental study of drop shape oscillations in liquid-liquid systems. *J. Fluid Mech.*, **115,** 453–475.

Volz, F. E., 1960: Some aspects of the optics of the rainbow and the physics of rain. *Physics of Precipitation,* H. Weickmann, Ed., Amer. Geophys. Union, 280–286.